Supplementary Information

Evaluation of MnO_X, Mn_2O_3, and Mn_3O_4 Electrodeposited Films for the Oxygen Evolution Reaction (OER) of Water

Alejandra Ramírez, Philipp Hillebrand, Diana Stellmach, Matthias M. May, Peter Bogdanoff and Sebastian Fiechter**

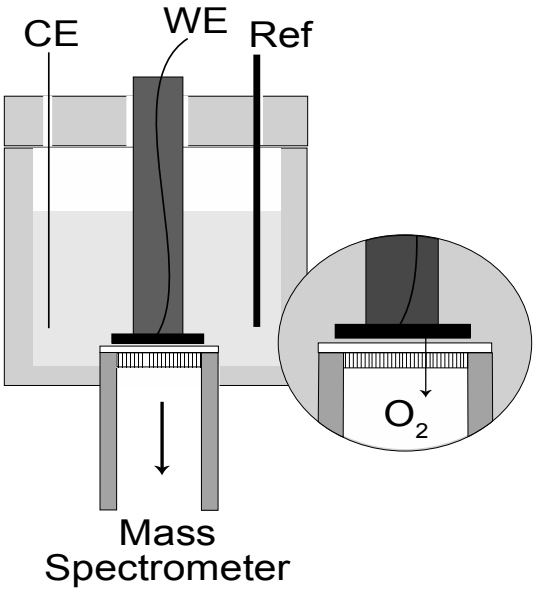

Figure S1. Electrochemical cell coupled with a differential electrochemical mass spectrometer (DEMS) used to characterize manganese oxide electrodes.

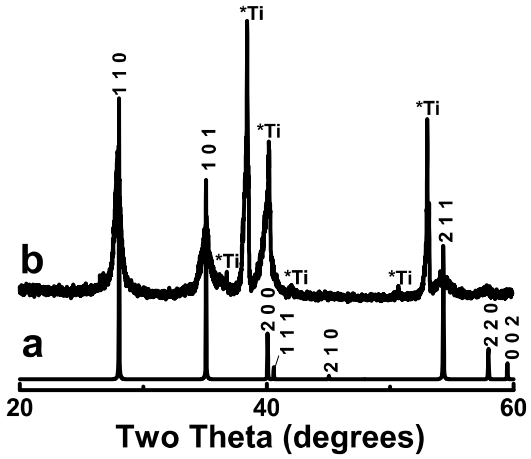

Figure S2. X-ray diffraction pattern of simulated RuO_2 (a) and sputtered RuO_2 on titanium metal (b).

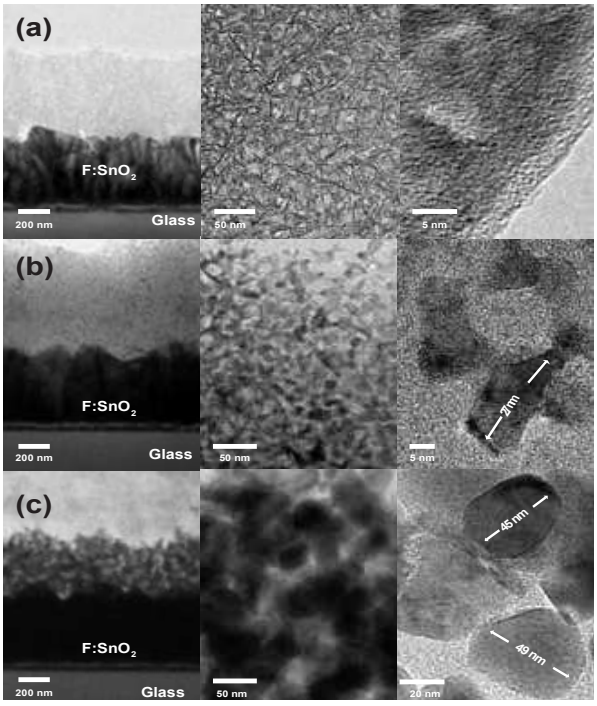

Figure S3. TEM cross-section images of MnO_x-373 K (a), α-Mn_2O_3 (b) and Mn_3O_4 (c) films deposited on F:SnO_2/glass.

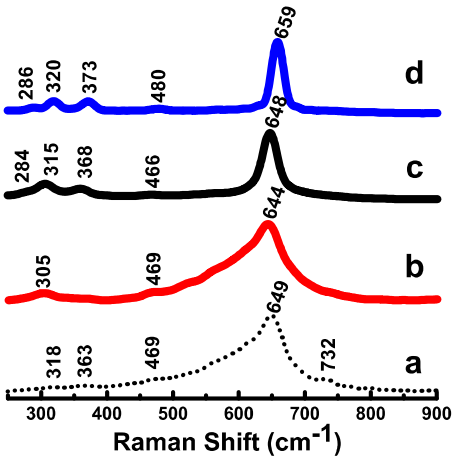

Figure S4. Raman spectra of MnO_x-373 K (a), MnO_x-573 K (b), α-Mn_2O_3 (c) and Mn_3O_4 (d) on F:SnO_2/glass.

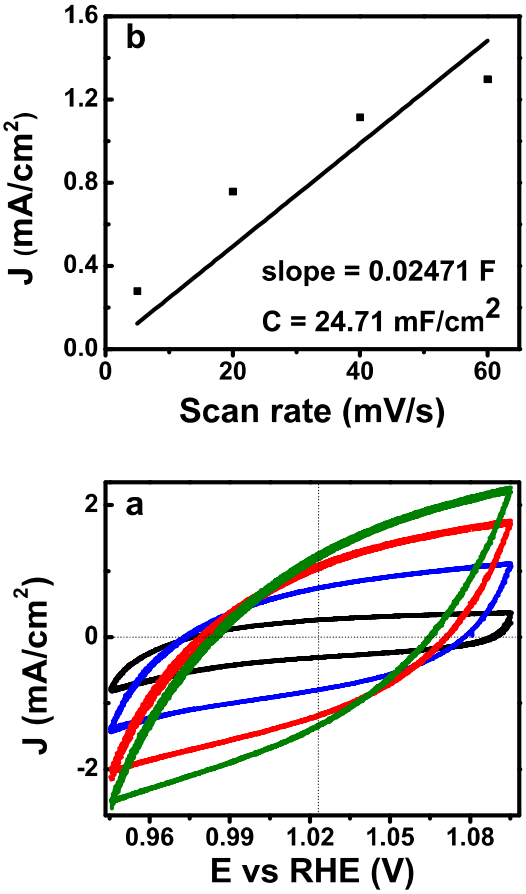

Figure S5. (a) Cyclic voltammograms of MnO_x-373 K (0.19 mg-1cm^2) film recorded at 5 mV/s (black), 20 mV/s (blue), 40 mV/s (red) and 60 mV/s (green). (b) Linear regression at 1.025 V vs. RHE in 1 M KPi.

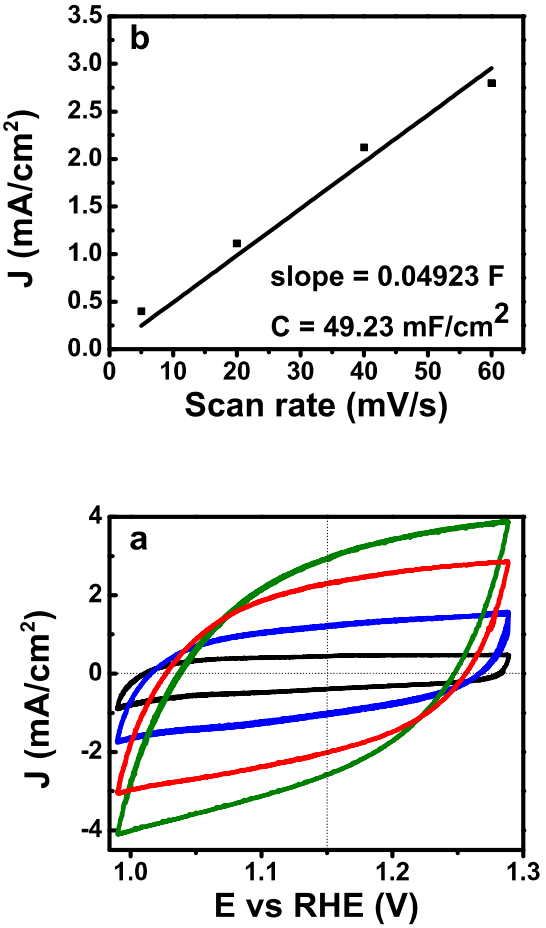

Figure S6. (a) Cyclic voltammograms of MnO_x-573 K (0.14 mg-1cm^2) film recorded at 5 mV/s (black), 20 mV/s (blue), 40 mV/s (red) and 60 mV/s (green). (b) Linear regression at 1.15 V vs. RHE in 1 M KPi.

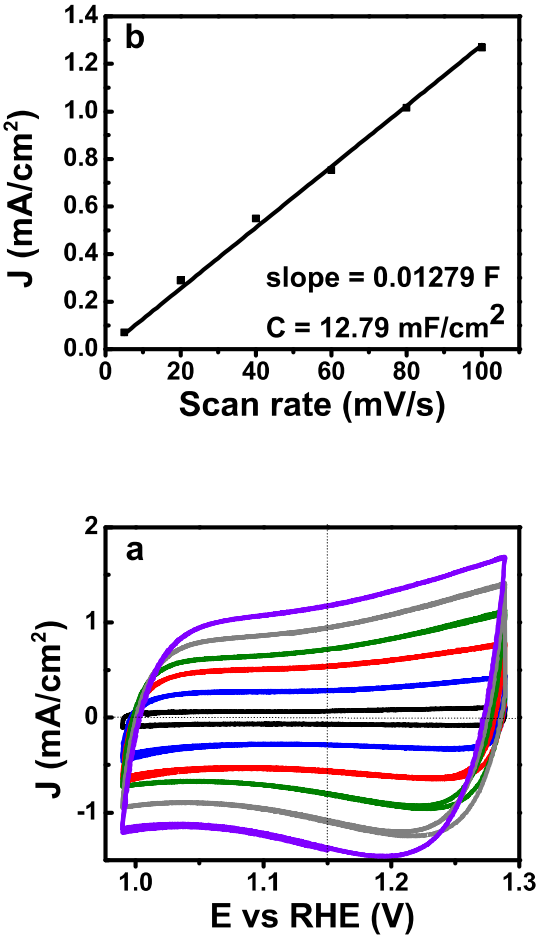

Figure S7. (a) Cyclic voltammograms of α-Mn_2O_3 (0.19 mg-1cm^2) film recorded at 5 mV/s (black), 20 mV/s (blue), 40 mV/s (red), 60 mV/s (green), 80 mV/s (gray) and 100 mV/s (purple). (b) Linear Regression at 1.15 V vs. RHE in 1 M KPi.

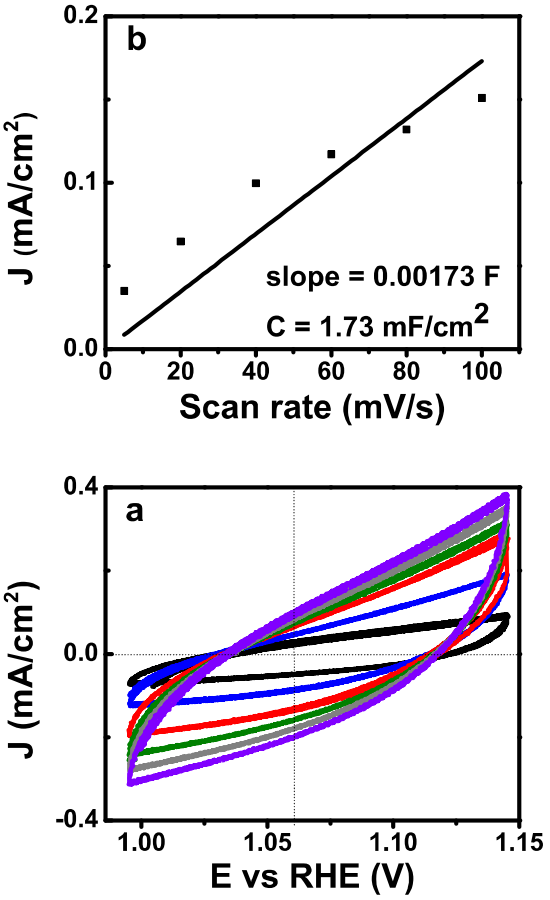

Figure S8. (a) Cyclic voltammograms of Mn_3O_4 (0.25 mg-1cm^2) film recorded at 5 mV/s (black), 20 mV/s (blue), 40 mV/s (red), 60 mV/s (green), 80 mV/s (gray) and 100 mV/s (purple). (b) Linear regression at 1.06 V vs. RHE in 1 M KPi.

Table S1. Summary of electrochemical values for MnO_x-373 K, MnO_x-573 K, α-Mn_2O_3, Mn_3O_4, sputtered RuO_2 (reference) and F:SnO_2/glass in neutral and basic solution.

Catalyst	OER[a)] [V]	J[b)] [mA/cm^2]	Pre-oxidation [V]
	1M KPi		
MnO_x-373 K	N/A	0.1	1.14 – 1.80
MnO_x-573 K	1.53	5.2	1.23 – 1.53
α-Mn_2O_3	1.47	6.7	1.13 – 1.47
Mn_3O_4	1.60	1.3	1.16 – 1.60
RuO_2	1.35	7.3	1.04 – 1.35
F:SnO_2	1.86	0	1.00 – 1.86
	1 M KOH		
MnO_x-373 K	N/A	N/A	N/A
MnO_x-573 K	1.46	18	0.9 – 1.46
α-Mn_2O_3	1.40	19	1.13 – 1.40
Mn_3O_4	1.52	7	1.16 – 1.52
RuO_2	N/A	N/A	N/A
F:SnO_2	1.62	0.5	1.00 – 1.62

[a)](OER vs. RHE at J = 0.1 mA/cm^2); [b)](J at η = 570 mV_{RHE})

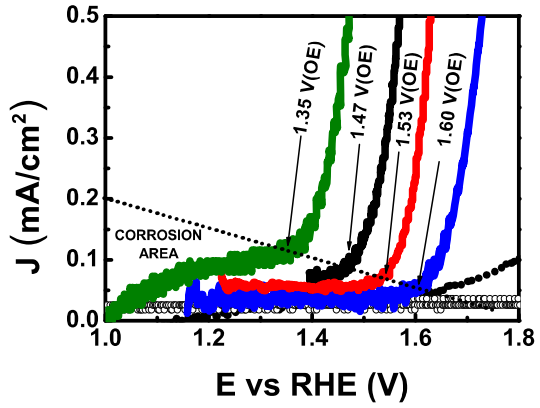

Figure S9. Current density vs. potential curve as a function of E vs. RHE of sputtered RuO_2 (green), MnO_x-373 K (dotted line), MnO_x-573 K (red), α-Mn_2O_3 (black) and Mn_3O_4 (blue) films deposited on F:SnO_2/glass (-○-) in 1 M KPi.

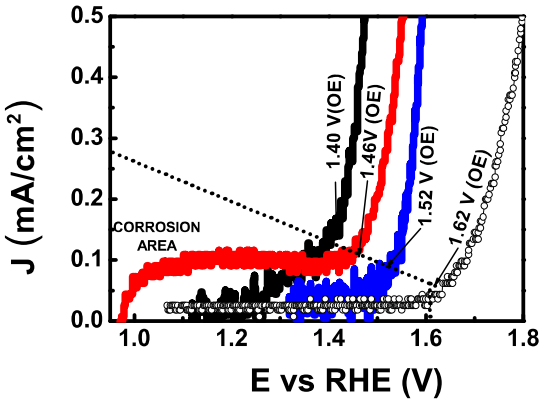

Figure S10. Current density vs. potential curve as a function of E vs. RHE of MnO_x-573 K (red), α-Mn_2O_3 (black) and Mn_3O_4 (blue) films deposited on F:SnO_2/glass (-○-) in 1 M KOH.

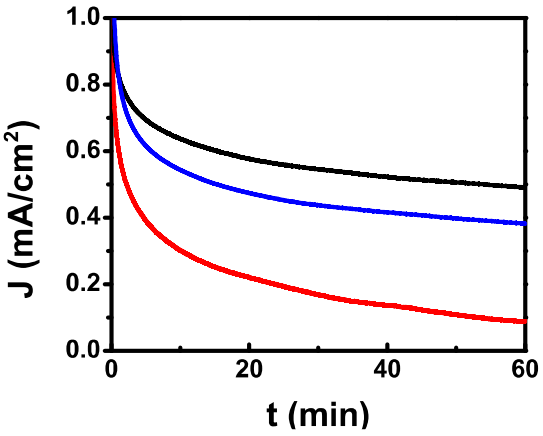

Figure S12. Normalized constant potential evaluation of MnO_x-573 K (red), α-Mn_2O_3 (black) and Mn_3O_4 (blue) electrodes in 1 M KPi at 1.7 V vs. RHE.

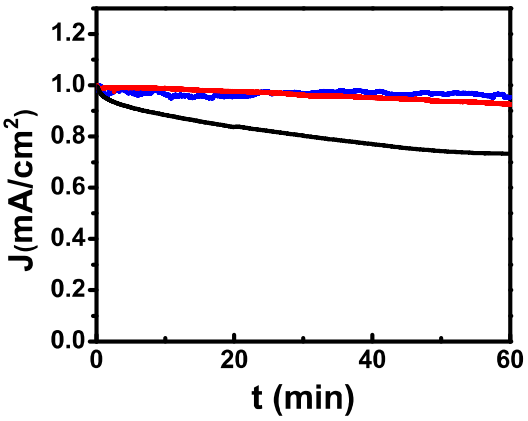

Figure S13. Normalized constant potential evaluation of MnO_x-573 K (red), α-Mn_2O_3 (black) and Mn_3O_4 (blue) electrodes in 1 M KOH at 1.7 V vs. RHE.

Table S2. XPS values of Mn $2p_{3/2}$, Mn $2p_{1/2}$ and O 1s for MnO_x-373 K, MnO_x-573 K, α-Mn_2O_3 and Mn_3O_4 films deposited on F:SnO_2/glass before electrochemistry (BE), high potential (HE) and low potential (LE) in neutral and basic solution.

Catalyst		Mn $2p_{3/2}$	Mn $2p_{1/2}$	O 1s	Mn (valence)
MnO_x-373 K	BE	642.2 (640.8, 641.7, 642.9)	653.8	530.0, 531.7	II, III, IV
MnO_x-573 K	BE	641.9 (641.4, 643.0)	653.5	529.5, 531.2	III, IV
α-Mn_2O_3	BE	641.3 (640.6, 641.6)	653.0	529.7, 531.3	II, III
Mn_3O_4	BE	641.0 (639.3, 640.2, 641.5)	652.8	530.0, 531.7	0, II, III
		1 M KPi			
MnO_x-573 K	HE	641.4, 642.6	653.5	529.0, 530.2, 532.9	III, IV
	LE	640.2, 641.5, 642.9	653.0	529.2, 530.7, 535.0	II, III, IV
α-Mn_2O_3	HE	641.4, 643.3	653.1	529.4, 530.5	III, IV
	LE	640.1, 641.4	652.8	529.2, 530.7	II, III
Mn_3O_4	HE	641.7, 642.7	653.5	529.5, 530.8	III, IV
	LE	641.8, 642.8	653.8	529.7, 531.1	III, IV
		1 M KOH			
MnO_x-573 K	HE	640.4, 641.9, 643.0	652.7	529.1, 530.7, 535.0	II, III, IV
	LE	640.0, 641.6, 643.0	652.1	528.7, 531.1, 532.2, 535.2	II, III, IV
α-Mn_2O_3	HE	641.6, 643.0	653.5	529.5, 530.8	III, IV
	LE	641.2, 642.9	653.3	529.5, 530.9, 532.6	III, IV
Mn_3O_4	HE	641.4, 642.9	653.4	529.3, 530.6, 532.3	III, IV
	LE	641.4, 643.0	653.3	529.4, 530.8, 533.0	III, IV

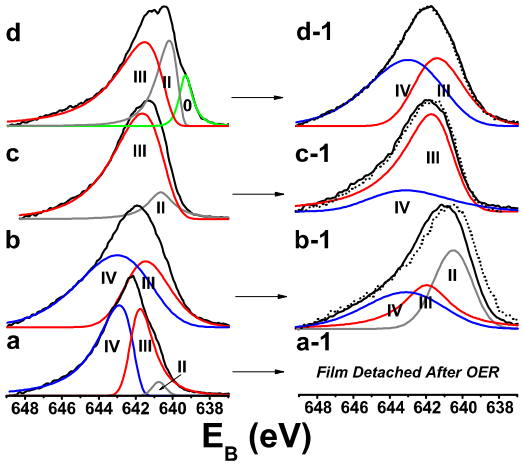

Figure S14. Deconvoluted XP spectra of Mn $2p_{3/2}$ before electrochemistry for MnO_x-373 K (a), MnO_x-573 K (b), α-Mn_2O_3 (c) and Mn_3O_4 (d) films deposited on F:SnO_2/glass. Deconvoluted XP spectra after OER (at ~1.8 V vs. RHE in 1 M KOH) for MnO_x-573 K (b-1), α-Mn_2O_3 (c-1), Mn_3O_4 (d-1) films and treatment at ~1.1 V vs. RHE (dotted line).

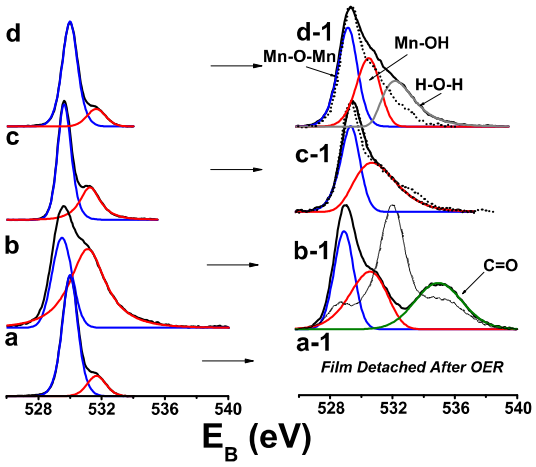

Figure S15. Deconvoluted XP spectra of O 1s before electrochemistry for MnO_x-373 K (a), MnO_x-573 K (b), α-Mn_2O_3 (c) and Mn_3O_4 (d) films deposited on F:SnO_2/glass. Deconvoluted XP spectra after OER (at ~1.8 V vs. RHE in 1 M KOH) for MnO_x-573 K (b-1), α-Mn_2O_3 (c-1), Mn_3O_4 (d-1) films and treatment at ~1.1 V vs. RHE (dotted line).

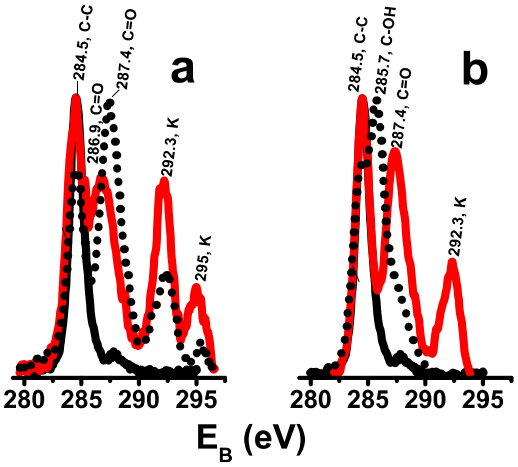

Figure S16. XP spectra of C 1s in 1M KPi (a) and 1 M KOH (b) for pristine MnO_x-573 K (black), after OER (at ~1.8 V vs. RHE in 1 M KOH) (red), after OER (at ~1.1 V vs. RHE in 1 M KOH) (dotted line).

Table S3. Structural parameters and A_{1g} Raman mode of different manganese oxides including Mn_4CaO_5 (cluster of photosystem II).

Manganese Oxide	Mn-O distance mean value [Å]	Mn-Mn distance shortest value [Å]	O-O distance shortest value [Å]	A_{1g} Raman mode [cm^{-1}]	Degree of covalency	Structure type
β-MnO_2	1.88_{oct}	2.87	2.87	667	73.6%	SnO_2
α-Mn_2O_3	2.04_{oct}	3.08	2.55	648	69.3%	Bixbyite (distorted)
Mn_3O_4	2.08_{oct}, 1.81_{tetr}	2.88	2.88	659	~70%	Spinel (distorted)
MnO	2.21_{oct}	3.30	3.14	-	29.5%	NaCl
$Mn(OH)_2$	2.26_{oct}	3.34	3.34	-	30%	CdI_2
Mn_4CaO_5	2.13_{cubane}	2.70	> 2.9	-	-	PS II